

Full rotational control of levitated silicon nanorods: supplementary material

STEFAN KUHN^{1,A,*}, ALON KOSLOFF^{2,A}, BENJAMIN A. STICKLER³, FERNANDO PATOLSKY², KLAUS HORNBERGER³, MARKUS ARNDT¹, AND JAMES MILLEN¹

¹University of Vienna, Faculty of Physics, VCQ, Boltzmannngasse 5, 1090 Vienna, Austria

²School of Chemistry, Tel-Aviv University, Ramat-Aviv 69978, Israel

³University of Duisburg-Essen, Lotharstraße 1, 47048 Duisburg, Germany

^ACo-First Authors

*Corresponding author: stefan.kuhn@univie.ac.at

Published 13 March 2017

This document provides supplementary information to “Full rotational control of levitated silicon nanorods,” <https://doi.org/10.1364/optica.4.000356>. We discuss the experimental methods to individually measure the various motional degrees of freedom of a trapped nanorod and present the theoretical framework for fitting this data. The scaling of the extracted trapping frequencies with the laser power is displayed. © 2017 Optical Society of America

<https://doi.org/10.1364/optica.4.000356.s001>

1. DISTINGUISHING DIFFERENT TRANSLATIONAL AND ROTATIONAL MOTIONS

All trapping frequencies of the nanorods can be calculated, based on their geometry as measured through scanning electron microscopy. The scattered light signal contains information about all degrees of freedom, with a high signal-to-noise ratio (SNR) [1]. In the manuscript, all data for (x, y, z, α) is extracted from the scattered light detector D4, and the motion in β is extracted from a polarization dependent measurement on the scattered light D5.

We independently check all motional degrees of freedom to confirm our assignation of frequencies, using other detectors. This information is not used in the manuscript. The full optical layout is shown in Fig. S1, and each detector and its uses are outlined in table S1.

Motion in z and α : We expect the trapping frequencies for z and α to be $f_z = 124$ kHz and $f_\alpha = 134$ kHz respectively. In the data we see a double-peak in the Power Spectral Density (PSD) of the scattered light signal D4 around these frequencies, as shown in Fig. S2a). To confirm experimentally which peak is which we implement an additional detection scheme. The nanorod rotates the polarization of the trapping light, depending on the angle it makes to the polarization axis (i.e. by an amount proportional to α).

We monitor the trapping light that has interacted with the nanorod by collecting some of the light coupled back into the fiber outcouplers, splitting it off with a 99:1 fiber beamsplitter

and turning its linear polarization by 45° . This light then goes through a fiber polarizing beamsplitter (PBS), and each arm of the PBS is coupled onto a fast fiber-coupled balanced detector D1 (Thorlabs PDB420C). By this method we measure just the rotation in α , as shown in Fig. S2a). This confirms that the higher frequency peak is due to motion in α .

We also monitor the intensity fluctuations of this picked-off light on detector D2, which yields information about the motion in z , as described in Ref. [2]. The quality of this signal is poor, due to the large beam waist of our trap, and could be improved through a difference measurement. It reconfirms that the peak at 124 kHz is due to motion in z .

Motion in x, y : We pick off a small amount of the light that has interacted with the nanorod using a free-space 97:3 beamsplitter. This light is incident on a D-shaped mirror to cut the beam in half, and the resulting two beams are measured on a differencing photodiode D3. This yields the motion in y , as described in Ref. [2]. By performing a half-waveplate operation on the trapping light we can rotate the nanorod to measure x . Due to the large beam waist of our trap, the SNR is poor for this signal.

Motion in β : Using a lens we collect the scattered light emitted in the opposite direction to that collected by the multimode fiber. This light is sent through a polarizing beamsplitter cube, which is rotated by 45° with respect to the x -axis, and monitored with a photodiode D5. This yields information about the motion in β , as shown in Fig. S2b).

Detector	Model	Motional sensitivity
D1	Fiber coupled differencing photodetector, Thorlabs PDB420C	α
D2	Fiber coupled photodetector Bookham PP-10GC58L	x, y, z
D3	Homebuilt differencing photodetector	x or y
D4	Multimode fiber coupled Hamamatsu photodiode G12180-005A with Femto HCA-100M-50K-C amplifier	All degrees of freedom
D5	Free space photodetector Thorlabs DET10C	β

Table S1. Detectors used to measure the motion of a levitated silicon nanorod. Only detectors D4 and D5 are used in the manuscript, D1-3 are used for confirming our assignment of motional degrees of freedom.

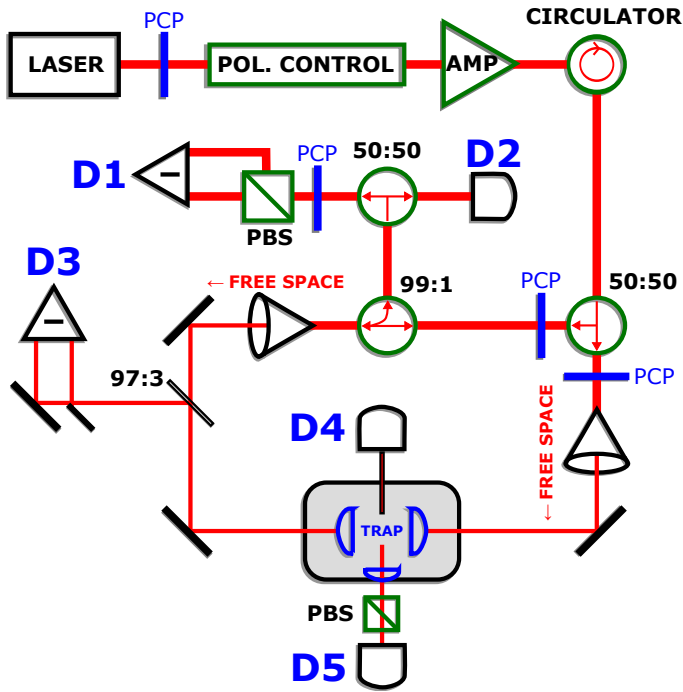


Fig. S1. The full optical layout, including mechanisms for independently measuring different trapping frequencies. A small portion of the free-space light is split on a D-shaped mirror, yielding the radial motion x on detector D3. A portion of the light that is coupled back into the fibers is picked off, and split equally to be sent to two detectors. D2 monitors the motion in z , as described in Ref. [2], and D1 the motion in α . We collect the light which the nanorod scatters using a multimode fiber, and monitor its intensity on detector D4, and use a lens to collect the scattered light to perform a polarization sensitive measurement in the 45° basis on detector D5.

Further notes on detection

The SNR from the scattered light detector D4 is significantly better than that from detectors D1,2,3. Because of this, even though the z and α peaks overlap, fitting the PSD of D4 is the most accurate method for monitoring the dynamics of the nanorod. However, we can always use the other detectors to confirm our findings. The SNR of the scattered light signal is so good because we only collect light that is scattered by the nanorod, with virtually zero background.

We expect the scattered light signal D4 to be only sensitive to the first harmonic of all motions $2f_{x,y,z,\alpha,\beta}$, since it depends on position squared. However, Fig. S2a) shows that we measure the fundamental motions $f_{z,\alpha}$ on D4. This is due to a slight misalignment between the trapping beams, and because the polarization in each arm of the trap is not perfectly identical. We confirm this through calculation, which also confirms that D4 is not sensitive to the fundamental frequency f_β .

The polarization (rather than intensity) sensitive detectors D1,5 are sensitive to the sign of the motion in α, β respectively, and so the PSDs in Fig. S2 show the frequency $f_{\alpha,\beta}$ and not its harmonic.

2. FITTING DATA

To extract trapping frequencies we fit the PSD of the scattered light time series with the function

$$\text{PSD}(\omega) = C_d^2 \frac{2k_B T}{M_d} \frac{\Gamma_d}{(\omega_d^2 - \omega^2)^2 + \omega^2 \Gamma_d^2}, \quad (\text{S1})$$

where d labels the degrees of freedom (i.e. x, y, z, α, β), Γ_d is the (angular) momentum damping rate, ω_d is the trapping frequency, M_d is the particle's mass or moment of inertia and C_d is the calibration between our measured signal and absolute motional information. The derivation of this PSD is standard, e.g. [2, 3]. When recording the time series of the particle's motion, the PSD can usually be calibrated to extract C and convert from units of $\text{V}^2 \text{Hz}^{-1}$ to $\text{m}^2 \text{Hz}^{-1}$. However, our signal contains both translational (x, y, z) and rotational (α, β) information, so such a global calibration isn't possible. As an indication of sensitivity, the peak sensitivity for motion in the z direction from the PSD from detector D4 is $3 \mu\text{m}^2 / \text{Hz}^{-1}$.

Each degree of freedom can be fit with this expression. Figure S3 shows an example of fitting the PSD. Due to the proximity of the z and α peaks in the scattered light PSD, we fit the data with a sum of two of the functions defined in Eq. S1 to extract the parameters for both the z and α motions.

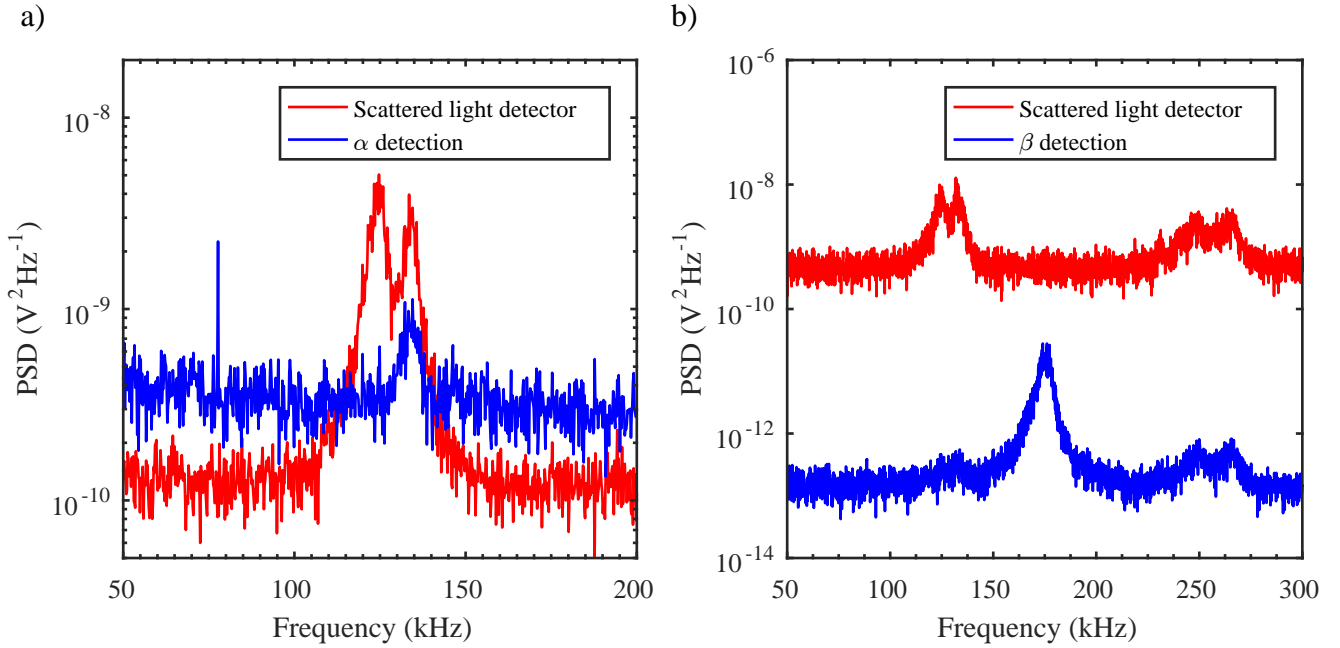


Fig. S2. a) A comparison of the PSD of the signal from the scattered light detector D4 (red), which is sensitive to motion in all directions, and the polarization sensitive detector D1 (blue), which is only sensitive to α . This confirms that the higher frequency peak corresponds to the α motion, which agrees with our calculations. b) A comparison of the PSD from the scattered light detectors D4 (red) and D5 (blue, polarization sensitive). D5 is sensitive to the frequency f_{β} , which isn't visible on detector D4.

3. TRAPPING FREQUENCY POWER SCALING

We expect all trapping frequencies to scale with the square root of power, see Eq. (1) of the manuscript. Figure S4 shows the measured trapping frequencies as a function of power in comparison to the theoretical expectation. The only unknown experimental parameter is the laser waist w_0 , which we extract from the ratio of f_z to f_x . The ratio of f_z to f_α confirms the length of our nanorod, which agrees with scanning electron microscope images. We observe excellent agreement between theory and $f_{\alpha,z}$, and also for the axial frequency when the rod is rotating $f_{z,\text{rot}}$. The discrepancy ($< 5\%$) between theory and experiment for f_β is attributed to the fact that the rods have finite diameter ($d = 130$ nm) and, the generalized Rayleigh-Gans approximation [4] is not strictly valid.

4. REDUCTION OF TRAPPING POTENTIAL WHEN THE PARTICLE IS ROTATING

Due to the rotation of the rod in the plane orthogonal to the trap axis, only the averaged susceptibility $(\chi_{\parallel} + \chi_{\perp})/2$ enters the trapping potential of the translational motion in z -direction. This means that in Eq. (1) of the manuscript, χ_{\parallel} has to be replaced by $(\chi_{\parallel} + \chi_{\perp})/2$. This agrees well with the measured reduction of the trapping frequency, see Fig. S4.

5. EXTRACTING INFORMATION FROM THE ROTATIONAL MOTION

When the trapping light is circularly polarized the nanorod rotates in the plane orthogonal to the trap axis (α direction) with the frequency $f_{\alpha,\text{rot}}$. As shown in the paper, $f_{\alpha,\text{rot}}$ has a broad distribution. To analyze this motion we extract the instantaneous frequency, using time bins 100 times longer than the mean rota-

tional period. In the paper we present the mean value of $f_{\alpha,\text{rot}}$ and display shaded regions around the data points representing the minimum and maximum values of $f_{\alpha,\text{rot}}$. The theoretical analysis predicts the maximum rotation frequency $f_{\alpha,\text{max}}$, which is determined by the balance between the torque exerted by the light field and the rotational friction due to collisions with gas molecules.

REFERENCES

1. S. Kuhn, P. Asenbaum, A. Kosloff, M. Sclafani, B. A. Stickler, S. Nimmrichter, K. Hornberger, O. Cheshnovsky, F. Patolsky, and M. Arndt, "Cavity-Assisted Manipulation of Freely Rotating Silicon Nanorods in High Vacuum." *Nano Lett.* **15**, 5604–5608 (2015).
2. Gieseler, J., Deutsch, B., Quidant, R. and Novotny, L., "Subkelvin Parametric Feedback Cooling of a Laser-Trapped Nanoparticle." *Phys. Rev. Lett.* **109**, 103603 (2012).
3. Millen, J., Deesuwan, T., Barker, P. F. and Anders, J., "Nanoscale temperature measurements using non-equilibrium Brownian dynamics of a levitated nanosphere." *Nature Nano.* **9**, 425 (2014).
4. Stickler, B. A., Nimmrichter, S., Martinetz, L., Kuhn, S., Arndt, M. and Hornberger, K., "Rotational Cavity Cooling of Dielectric Rods and Disks." *Phys. Rev. A* **94**, 033818 (2016).

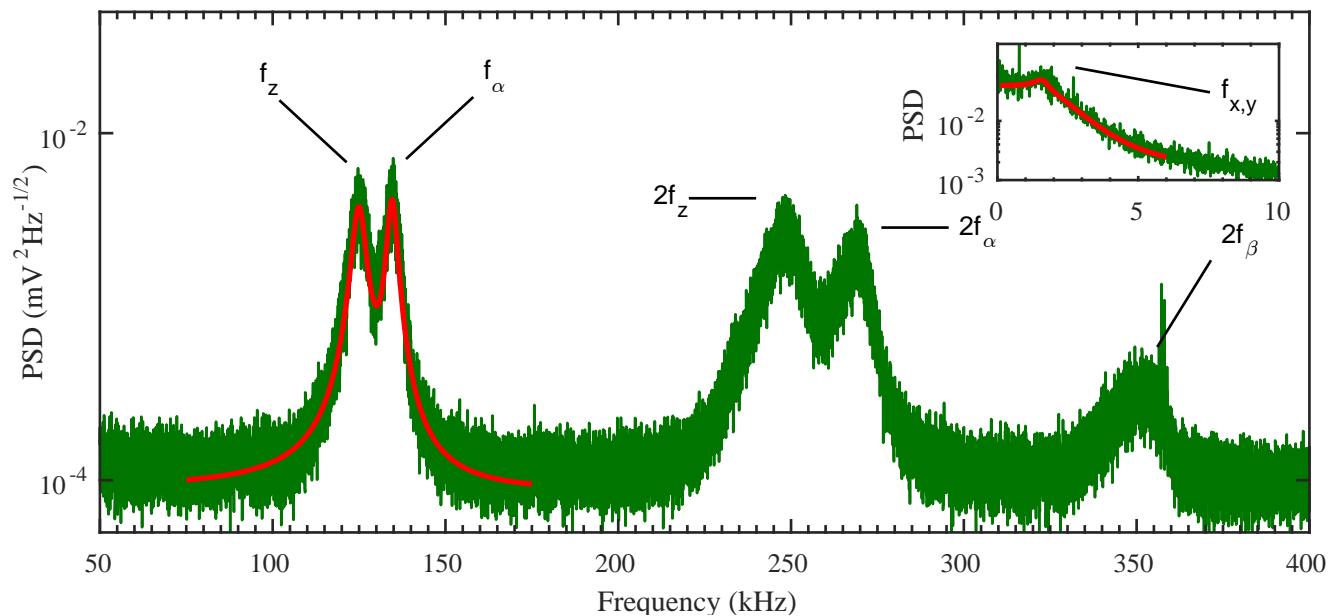


Fig. S3. The PSD of the scattered light signal showing all motional degrees of freedom. Solid red lines are fits to the data using Eq. S1.

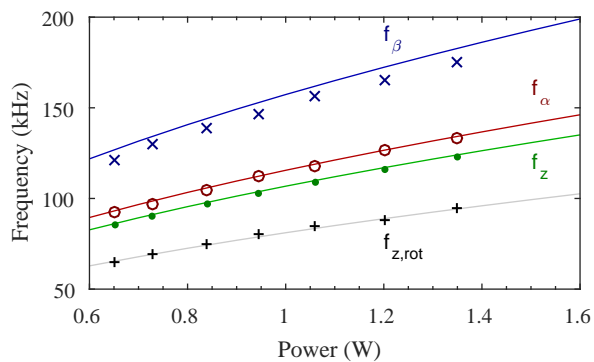


Fig. S4. Variation in the trapping frequencies with total trap power, markers are data, solid lines are the theoretical predictions. The frequency $f_{z,rot}$ is the trap frequency in the z direction when the nanorod is rotating in the α direction. Experimental uncertainties are smaller than the data markers.